A Micromechanics Analysis of Nanoscale Graphite Platelet-Reinforced Epoxy Using Defect Green's Function

B. Yang[1,2], S.-C. Wong[3] and S. Qu[3]

Abstract: In the modeling of overall property of composites, the effect of particle interaction has been either numerically taken into account within a (representative) volume element of a small number of particles or neglected/ignored in order for efficient solution to a large system of particles. In this study, we apply the point-defect Green's function (GF) to take into account the effect of particle interaction. It is applicable to small volume fractions of particles (within 10 %). The high efficiency of the method enables a simulation of a large system of particles with generally elastic anisotropy, arbitrary shape and composition, and arbitrary spatial distribution. In particular, we apply the method to study the nanoscale graphite platelet reinforced polymers, guided by some preliminary experimental observations. We first verify the method by comparing the prediction with a full-field model in the case of a regular lattice of particles. The comparison has demonstrated that the method is a considerable improvement over the classical Eshelby's method employing the regular GF and thus ignoring the effect of particle interaction. Upon the verification, we apply the method to examine the effect of a number of parameters on the overall composite behavior. The effect of particle interaction is shown to be strongly dependent on particle arrangement due to the strong elastic and geometrical anisotropy in graphite platelets. The strongest effect occurs when the platelets are oriented uniformly and stacked in a simple cubic lattice. However, the (overall) effect becomes trivial when the platelets are randomly orientated, which is expected. The effect of platelet aspect ratio is also studied. Finally, a thin soft layer is inserted between the platelets and the matrix material in order to simulate a partial bonding condition between them. It is shown to play a significant role in determining the overall composite behavior. The present work sets up a base for further large-scale simulations of micro-damages (microcracks, particle debonding, etc.) under interaction, as well as providing insights to further experimentation in graphite platelet nanocomposites.

1 Introduction

Various micromechanics models have been developed to estimate the overall elastic property of particle-reinforced composites (Mura, 1987; Nemat-Nasser and Hori, 1999). They are exclusively based on the average stress and strain over a representative volume element (RVE), which supposedly contains a sufficiently large number of particles. These models may be classified in two categories: (a) analytical, based on approximate but efficient solutions of stress and strain fields in a large RVE; (b) numerical, based on numerical full solutions of stress and strain fields in a small RVE. For an accurate evaluation, the full stress and strain fields are in general needed. The numerical methods commonly used to solve the problem include the finite element (FE) method and the boundary element (BE) method. The FE method has so far been limited to a small RVE of a few tens of particles with the current

---

[1] Corresponding author. Tel: 321-674-7713, Fax: 321-674-8813, Email: boyang@fit.edu

[2] Department of Mechanical and Aerospace Engineering, Florida Institute of Technology, Melbourne, FL 32901

[3] Department of Mechanical Engineering, University of Akron, Akron, OH 44325

computing powers (LLorca and Segurado, 2004). The BE method is based on a boundary-integral-equation formation employing Green's functions (GFs) (Brebbia et al., 1984). The BE method based on analytical/semi-analytical GFs reduces problem dimensionality by one and holds flexibility for further mesh reduction and efficiency improvement by realizing certain features of a problem (Pan et al., 2001). For example, if the particles are rigid, the number of degrees of freedom (DOFs) can be cut by one half. Depending on the characteristics of a GF, a fast multipole scheme may be devised to accelerate the solution. Therefore, the BE method has been ably extended to handle a RVE of thousands of fibers on parallel computers (Liu et al., 2005). However, it is yet unclear how to extend the approach to a more complicated case of generally elastic fibers and particles where the above analytical treatments may not be readily available.

Due to the limitation of numerical methods, various analytical methods have been developed and favored historically for the estimate of overall elastic property of particle-reinforced composites (Mura, 1987; Nemat-Nasser and Hori, 1999). In the early studies, a uniform stress or a uniform strain field was assumed throughout the entire composite system. These approaches were later proved to provide an upper and a lower bound of overall elastic stiffness, respectively. In a more accurate approach, namely, the Eshelby's method, the full stress and strain fields are approximated by the sum of those due to individual particles separately in an infinite matrix (Eshelby, 1961; Mura, 1987). The problem may be analytically dealt with as an equivalent inclusion problem and solved conveniently with GFs. It is applicable to composites of dilute particles since it does not take into account the effect of particle interaction. The self-consistent method (Budiansky and Wu, 1962) takes into account the effect of particle interaction in a plausible way by considering the problem of particles embedded in an assumed homogeneous matrix. The overall elastic property of the assumed matrix plus the particles is evaluated by the Eshelby's method. If there appears to be little change in the overall elastic property,

the assumed matrix is regarded as equivalent to the composite under consideration. That is that the elastic property of the composite is obtained. An iterative scheme is necessary to solve the self-consistent problem starting with the original matrix. In the approach the stress and strain fields are captured remote to each particle in an average sense. However, they are in serious question in the vicinity of each particle. Therefore, it is difficult to estimate the accuracy of the method. The embedded cell method (Dong and Schmauder, 1996) advances over the original self-consistent method, which resolves the stress and strain fields in the vicinity of individual particles in a cell of original matrix while wrapping the cell with a homogeneous material of the same (initially unknown) elastic property of the composite. The problem is solved iteratively, the same as in the original self-consistent method. It offers an accurate evaluation of the overall elastic property of the composite. However, the method would normally require the use of a numerical solver, limiting its application to small RVEs (Okada et al., 2004).

In this paper, a novel analytical method is developed to estimate the overall elastic property of particle-reinforced composites by using defect GF. The defect GF is basically the field due to a unit point force in a matrix containing inhomogeneous particles, namely, defects (Yang and Tewary, 2004). In contrast, the regular GF is referred to the field due to a unit point force in a homogeneous matrix. When the defect GF is applied to derive the stress and strain fields, the effect of particle interaction is taken into account. An efficient scheme has been developed for evaluation of the defect GF of point-like inhomogeneities (in a multilayered matrix in general) (Yang, 2004). By assuming particles being point-like and applying the point-defect GF, an analytical method is obtained, capable of simulating a large system of particles. It allows for efficient and accurate examination of the effects of various parameters, such as particles geometry and orientation, on the overall property of the composite.

The present modeling work is motivated by our recent attempt to develop a novel graphite platelet-reinforced polymer system (Zheng et al.,

2002; Zheng and Wong, 2003; Zheng et al., 2004; Wong et al., 2004, 2005; Wong and Yang, 2005). The concept was novel because little was understood on dispersing exfoliated graphite platelets in polymers. Graphite intercalated compounds (GICs) have been studied for a few decades (Chung, 1987; Toyoda and Inagaki, 2000; Yoshida et al., 1991). New patents (Barsukov and Zaleski, 2004; Jang et al, 2004) and research findings (Qu and Wong, 2005; Wong et al., 2006) on novel processing methods to produce highly expanded graphite continue to emerge. However, the advantages of dispersing GIC in polymers to formulate novel nanocomposites are not well understood. Widespread interests arose in dispersing various nanoscale fillers including carbon nanotubes (Gong et al., 2000; Thostenson and Chou, 2002) and organomodified smectite clays (Kojima et al., 1993; Giannelis et al., 1999) in polymers. Little has been reported on dispersing nanoscale graphite platelets (NGPs), which consist of stacks of sp^2 graphene sheets in polymers, and their treatment methods. Such an NGP-based polymer nanocomposites are distinctly different from those obtained from conventional sp^3 carbon black, carbon nanotube and nanoclay reinforcements. Instead of developing the lower-cost processes for fabrication of nanotubes, we studied experimentally the use of platelet-shaped graphite, which exists abundantly in our planet earth, coupled with mechanical attrition processes (Wong et al., 2006) to produce low-cost nanoscale substitutes that provide attractive functional properties when dispersed in polymer matrices. The functional properties include improved mechanical stiffness, ductility, electrical conductivity, dielectric and piezoresistive properties that are the focus of our research (Zheng et al., 2002; Zheng and Wong, 2003; Zheng et al., 2004; Wong et al., 2004, 2005; Wong and Yang, 2005; Wong et al., 2006). The general advantages of nanoscale reinforcements in polymer matrices are threefold: (1) when nanoscale fillers are finely dispersed in the matrix, the tremendous surface area developed could contribute to polymer chain confinement effects which could lead to higher glass transition temperature, stiffness and strength; (2) nanoscale fillers provide an extraordinarily zigzagging, tor-

tuous diffusion path that leads to enhanced barrier performance for gas, moisture and oxygen transmissions; and (3) nanoscale fillers can also enhance the controlled electrical and thermal conductivities to finely tune insulating, dielectric and semi-conductive properties. Advantage (3) cannot be effectively obtained from nanocomposites derived from layered silicates. In this paper, we focus on the elastic mechanical properties.

In Section 2, some preliminary experimental results of graphite platelets epoxy nanocomposites are described. They provide guiding parameters for the following modeling and simulations. In Section 3, the novel defect GF-based analytical method is described. In Section 4, the present method is first verified to predict accurately compared to the full-field solution in the case of a regular lattice of particles. Then, a parametric study is carried out to investigate the role of a number of parameters in determining the overall elastic property of composite. It is found that the particles orientation, geometry and distribution all play a significant role in general. The effect of particle interaction is significant when the graphite platelets are aligned with their c-axis and in a simple cuboidal lattice. However, it becomes trivial overall when the platelets are randomly orientated. High aspect ratio of platelets is desired for better stiffening effect. In addition, the effect of a soft thin layer simulating partial bonding condition between the particles and matrix material is studied. In Section 5, conclusions are drawn.

2 Experiments

Scanning Electron Microscopy (SEM) was used to examine the expanded and undispersed graphite platelets. Samples were placed on aluminum sample studs using double sided carbon tape. To avoid electron charging and ensure quality imaging SEM samples were sputter coated with gold prior to observation. Dispersed graphite in epoxy was examined using a transmission light microscope (Fisher Scientific Micromaster I) of microtomed sections.

A Nicomp 380 Submicron Particle Size Analyzer was used to measure the sizes of the undispersed graphite platelets. The instrument uses Dynamic

Light Scattering (DLS), also known as the Photon Correlation Spectroscopy (PCS), to obtain the particle size distribution for samples with particles that can range from 1 nm to 5 μm. According to the manufacturer, the proprietary Nicomp analysis algorithm is able to analyze complex multimodal distributions with the industrial highest resolution and reproducibility available. It is an absolute measurement, where knowledge of composition of the suspended particles is not required. Graphite platelets were dispersed in distilled water and methyl alcohol solution at a 50:50 ratio. The solution was then diluted with more water-alcohol solution so that the solution had only a slight gray tint, but yet transparent. The diluted graphite solution in a glass tube was placed into the particle size analyzer sample cell. Results were plotted using the Nicomp 380 Analyzer module.

The early work by Wong and coworkers (Zheng et al., 2002; Zheng and Wong, 2003; Zheng et al., 2004; Wong et al., 2004, 2005; Wong and Yang, 2005; Wong et al., 2006) focused on the chemical treatments required to expand and exfoliate graphite sublayers (plates or stacks of graphene planes) in generating nanoscale fillers. It was found that the percolation threshold for electrical conductivity was markedly reduced with acid treatment as a function of acid treatment time. Natural graphite materials provide good electrical conductivity (10^6 S/m at ambient temperature) and layered structure with a *c*-axis lattice constant, which indicates interplanar spacing, of 0.34 nm (Cao et al., 1996) when expanded. Using a proper design of acid treatment, graphite sublayers could be greatly expanded. Figure 1a shows original, untreated graphite flakes under the scanning electron microscope (SEM). After acid treatment, the electron beam focuses on the nanoscale feature of the sheet edge of graphite platelet, as shown in Figure 1b. Evidently, the graphitic domains have been drastically reduced in thickness, from several micrometers to 100 nanometers and less. Note that Figure 1a shows the well-known expanded graphite morphology that is undispersed. The structures produced as shown in Figure 1 can be ground to smaller platelets us-

ing ball milling (Wong et al., 2006) or homogenizer.
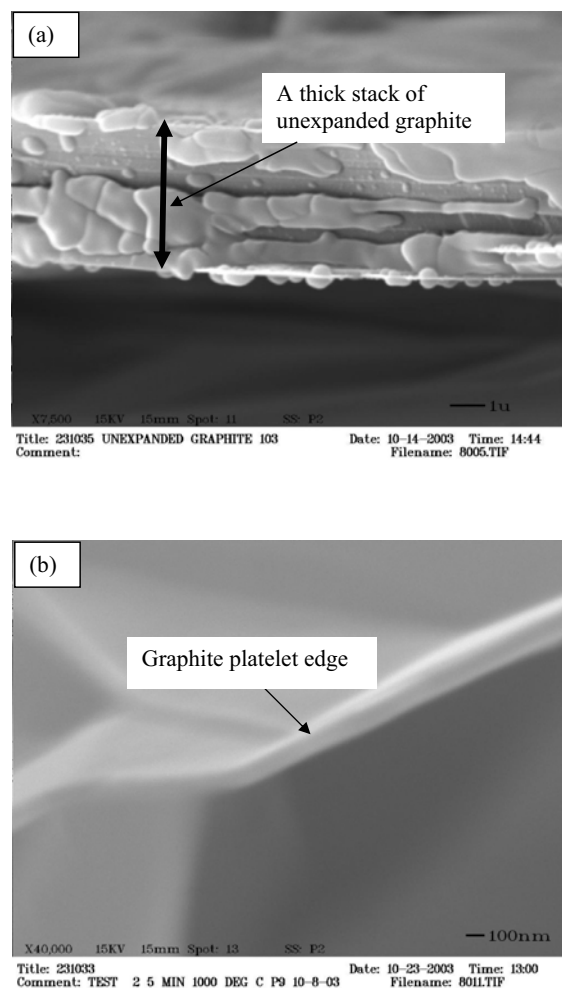
Figure 1: (a) SEM photomicrograph of a natural flake graphite; (b) enlarged nanoscale feature ($\sim$100 nm): sheet edge.

Figure 2 shows the platelet size distributions plotted by the Nicomp 380 Submicron Particle Size Analyzer after a ball milling process. The particle sizing uses DLS and works by first measuring the scattered light intensity at one angle. The intensity of light scattered in a particular direction by dispersed particles tends to periodically change with time. These fluctuations in the intensity vs. time profile are caused by the constant changing of particle positions brought on by the Brownian motion. DLS instruments obtain, from the intensity vs. time profile, a correlation

function. This exponentially decaying correlation function is analyzed for characteristic decay times, which are related to the diffusion coefficients and then by the Stokes-Einstein equation, to the particle radius. The DLS approach is able to identify particles ranging from 1 nm to 5 microns reliably and reproducibly. It is also better than other laser light scattering techniques available. It is noted that two major distributions occur. This is attributed to two contributing factors: (1) there exist two dimensions (edge thickness and platelet width) being targeted in the analyzer and (2) the distribution of submicron-sized particles in addition to nanoscale particles. It is clear that the edge thickness dimension is in the range of 100 nm while the platelet width is over 400 nm. The size distribution is generally consistent with the platelet shape as examined by microscopic techniques. The modeling dimensions reported herewith are aligned with the experimental observation we made after ball milling.
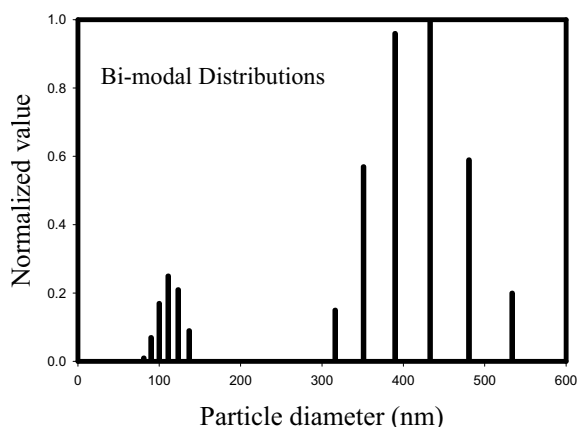
Figure 2: Bimodal distribution of micron-sized and nano-sized dimensions of nanoplatelets and their agglomerates.

The platelet dispersion in epoxy without ball milling but with homogenizing sonication was also examined. Figure 3 illustrates the dispersion of homogenized graphite flakes in epoxy resins. The dispersion of graphite platelets in thermosetting polymers appears uniform. The optimization in dispersion uniformity and mechanical properties can be further enhanced by other experimental techniques such as chaotic mixing (Sau and

Jana, 2004) and surface treatment using UV/O$_3$ (Li et al., 2005) in our future work.
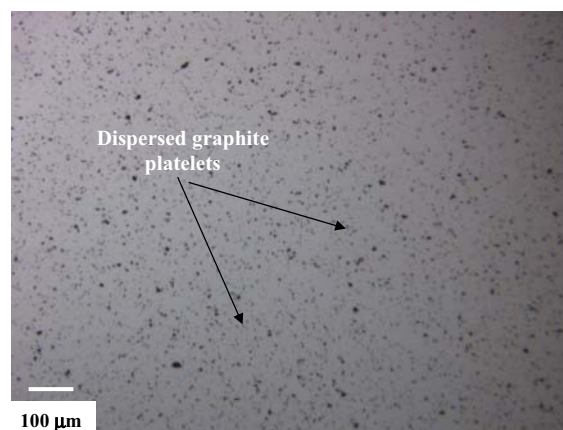
Figure 3: Optical micrograph of uniformly dispersed graphite platelets following sonication in an epoxy coating.

3 Defect Green's Function Method

Polymer nanocomposites reinforced by exfoliated nanoclay platelets and CNT were modeled by other investigators in recent years (Wu et al., 2004; Zhu and Narh, 2004; Fornes and Paul, 2003; Thostenson and Chou, 2003). The challenges for modeling polymer nanocomposites generally include: (a) characterization of molecular structure of the nanoscale fillers; (b) prediction of effective mechanical properties; (c) identification of optimized nanoscale configurations; (d) prediction of bulk mechanical properties of the composites; (e) modeling of the interfaces between nanoscale fillers and the matrix material; and (f) development of the models that bridge the hierarchy of length scales. In this paper, a novel micromechanical model is developed for estimate of the overall elastic property of graphite platelet-reinforced epoxy nanocomposite. The graphite platelets are assumed to be dilute and modeled as point-like inhomogeneous inclusions perfectly bonded to the matrix. The defect GF recently developed by Yang and Tewary (2004) and Yang (2004) is employed to solve the stress and strain fields and hence predict the overall elastic property of the composite. The method takes into ac-

count the effect of particle interaction. It is capable of dealing with arbitrary particles, including interfacial damage, point defects, etc., which may play an important role in determining the overall elastic property of nanocomposites with a large surface-to-volume ratio.

Nanoscale Graphite Platelets
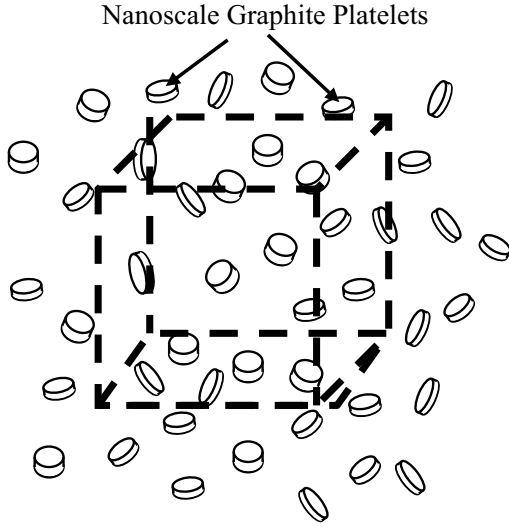
Figure 4: Schematic of a representative volume element (RVE) filled with and surrounded by particles.

In the modeling effort, two systems are considered: (a) a reference matrix, and (b) a composite material with embedded inhomogeneous particles. The composite material is schematically shown in Figure 4. The GF of the matrix in the absence of particles is termed as the reference GF, $\boldsymbol{G}$. The GF of the composite system is termed as the defect GF, $\boldsymbol{G}^*$. Yang and Tewary (2004) showed that these two GFs can be related through the continuum Dyson's equation. In the case of inhomogeneous particles, it is given by

$$G^*_{pi}(\boldsymbol{X}, \boldsymbol{x}) = G_{pi}(\boldsymbol{X}, \boldsymbol{x}) + \sum_n \int_{D_n} G^*_{pk,j}(\boldsymbol{X}, \boldsymbol{x}') \Delta C_{jkst}(\boldsymbol{x}') G_{si,t}(\boldsymbol{x}', \boldsymbol{x}) dV(\boldsymbol{x}'),$$
(1)

where $\boldsymbol{X}$ and $\boldsymbol{x}$ are the source and field points, respectively, D_n is the subdomain of the nth particle, and $\Delta \boldsymbol{C}^{(n)} (\equiv \boldsymbol{C}^0 - \boldsymbol{C}^{(n)})$ is the difference of elastic constants between the nth particle and the

matrix material. $\boldsymbol{C}^0$ and $\boldsymbol{C}^{(n)}$ are the elastic stiffness matrices of the matrix and the nth particle, respectively. Let us impose identical remote loading upon the reference and the defect systems. By multiplying the loading on both sides of Equation (1) and differentiating the resulting displacement, one may derive the following equation:

$$\varepsilon_{pq}(\boldsymbol{X}) = \varepsilon_{pq}^\infty + \sum_n \frac{1}{2} \int_{D_n} \Big(G^*_{pg,hq}(\boldsymbol{X}, \boldsymbol{x}) + G^*_{qg,hp}(\boldsymbol{X}, \boldsymbol{x}) \Big) \Delta C^{(n)}_{ghst}(\boldsymbol{x}) \varepsilon_{st}^\infty dV(\boldsymbol{x}), \quad (2)$$

which relates the strain field $\boldsymbol{\varepsilon}$ in the defect system to the strain field $\boldsymbol{\varepsilon}^\infty$ in the reference system. The (infinitesimal) strains $\boldsymbol{\varepsilon}$ are related to displacement $\boldsymbol{u}$ by $\varepsilon_{pq} \equiv \frac{1}{2}(u_{p,q} + u_{q,p})$. Since the reference system is homogeneous, $\boldsymbol{\varepsilon}^\infty$ is uniform. It may be worthwhile mentioning that there may be eigenstrain/eigenstress in the particles due to thermal residual stress and/or nonlinear deformation. However, its addition must not alter the overall elastic stiffness of the composite material under the small-strain condition and hence it is not considered here.

The overall elastic property of the composite is evaluated by averaging the stress and strain fields over a RVE containing a sufficiently large number of particles, as shown in Figure 4. It is supposedly surrounded by a sufficiently large number of particles as well. The effective strain is defined to be the volume average of strain within the RVE,

$$\langle \varepsilon_{pq} \rangle = \varepsilon_{pq}^\infty + \frac{1}{V} \int_V \sum_n \frac{1}{2} \int_{D_n} \Big(G^*_{pg,hq}(\boldsymbol{X}, \boldsymbol{x}) + G^*_{qg,hp}(\boldsymbol{X}, \boldsymbol{x}) \Big) \Delta C^{(n)}_{ghst}(\boldsymbol{x}) \varepsilon_{st}^\infty dV(\boldsymbol{x}) dV(\boldsymbol{X}), \quad (3)$$

with

$$\langle \varepsilon_{pq} \rangle = \frac{1}{V} \int_V \varepsilon_{pq} dV \quad (4)$$

where V is the volume of the RVE. By applying the divergence theorem, Equation (3) is rewritten as

$$\langle \varepsilon_{pq} \rangle = \varepsilon_{pq}^\infty + \frac{1}{V} \int_S \sum_n \frac{1}{2} \int_{D_n} \Big(G^*_{pg,h}(\boldsymbol{X}, \boldsymbol{x}) n_q(\boldsymbol{X}) + G^*_{qg,h}(\boldsymbol{X}, \boldsymbol{x}) n_p(\boldsymbol{X}) \Big) \Delta C^{(n)}_{ghst}(\boldsymbol{x}) \varepsilon_{st}^\infty dV(\boldsymbol{x}) dS(\boldsymbol{X}), \quad (5)$$

where S is the RVE surface, and $\boldsymbol{n}$ is the outward normal vector at a point on S. Assuming that $\boldsymbol{X}$ (a point on the RVE surface) is remote to all particles and that these particles are remote to each other, the above equation can be reduced as

$$\langle \varepsilon_{pq} \rangle = \varepsilon_{pq}^{\infty} + \sum_n I_{pqgh}^{*(n)} \int_{D_n} s_{ghkj}^{(n)} \Delta C_{jkst}^{(n)} \varepsilon_{st}^{\infty} dV, \quad (6)$$

with

$$I_{pqgh}^{*(n)} = \frac{1}{V} \int_S \frac{1}{2} \Big(G_{pg,h}^{*(-n)}(\boldsymbol{X}, x^{(n)}) n_q(\boldsymbol{X}) + $$
$$G_{qg,h}^{*(-n)}(\boldsymbol{X}, x^{(n)}) n_p(\boldsymbol{X}) \Big) dS(\boldsymbol{X}), \quad (7)$$

where $\boldsymbol{x}^{(n)}$ is the location of the nth particle, given in the average sense, e.g., the centroid of the particle, $G_{pg,hq}^{*(-n)}(\boldsymbol{X}, x^{(n)})$ is the less-defect GF in the presence of all particles but the nth one, and $s_{ghkj}^{(n)}$ is a tensor transforming the field at point $\boldsymbol{x}$ before and after the insertion of the nth particle. The tensor $s_{ghkj}^{(n)}$ satisfies the following equation,

$$s_{ghil}^{(n)}(\boldsymbol{x}) = \delta_{gi}\delta_{hl} + $$
$$\int_{D_n} s_{ghjk}^{(n)}(\boldsymbol{x}') \Delta C_{jkst}^{(n)}(\boldsymbol{x}') G_{si,lt}^{(}\boldsymbol{x}',\boldsymbol{x}) dV(\boldsymbol{x}'). \quad (8)$$

The less-defect GF $G_{pg,h}^{*(-n)}(\boldsymbol{X}, x^{(n)})$ satisfies the following equation,

$$G_{pi,l}^{*(-m)}(\boldsymbol{X}, \boldsymbol{x}^{(m)}) = G_{pi,l}(\boldsymbol{X}, \boldsymbol{x}^{(m)}) + $$
$$\sum_{n \neq m} G_{pg,h}^{*(-n)}(\boldsymbol{X}, \boldsymbol{x}^{(n)}) T_{ghst}^{(n)} G_{si,lt}^{(}\boldsymbol{x}^{(n)}, \boldsymbol{x}^{(m)}), \quad (9)$$

with

$$T_{ghst}^{(n)} = \int_{D_n} s_{ghjk}^{(n)} \Delta C_{jkst}^{(n)} dV. \quad (10)$$

Given $\boldsymbol{G}$, these equations can be solved to find $s_{ghkj}^{(n)}$ and $G_{pg,h}^{*(-n)}(\boldsymbol{X}, x^{(n)})$ (Yang, 2004).

The effective stress is evaluated by averaging the traction over the RVE surface S in each axis (instead of by averaging the stress field over the RVE volume). The present definition of effective stress is consistent with how the stress tensor is typically defined over an infinitesimal material element. It quantifies the amount of forces transmitted through the element surfaces. Similarly to the

above, by assuming that all the particles are remote to S as well as remote to each other, the effective stress may be derived from Equation (2) as

$$\langle \sigma_{pq} \rangle = C_{pqst}^0 \varepsilon_{st}^{\infty}$$
$$+ C_{pquv}^0 \sum_n J_{uvgh}^{*(n)} \int_{D_n} s_{ghkj}^{(n)} \Delta C_{jkst}^{(n)} \varepsilon_{st}^{\infty} dV, \quad (11)$$

with

$$\langle \sigma_{pq} \rangle = \frac{1}{2S_p} \int_S n_p(\boldsymbol{X}) n_r(\boldsymbol{X}) \sigma_{rq}(\boldsymbol{X}) dS(\boldsymbol{X})$$
$$\text{(no summation over p),} \quad (12)$$

$$C_{pquv}^0 J_{uvgh}^{*(n)} =$$
$$\frac{1}{2S_p} \int_S n_p(\boldsymbol{X}) n_r(\boldsymbol{X}) C_{rquv}^0 G_{ug,hv}^{*(-n)}(\boldsymbol{X},\boldsymbol{x}^{(n)}) dS(\boldsymbol{X})$$
$$\text{(no summation over p),} \quad (13)$$

where S_p is the projected area of the RVE in the plane normal to the pth axis, and $G_{pg,hq}^{*(-n)}(\boldsymbol{X}, x^{(n)})$ can be obtained by differentiating Equation (9) and solving the resulting equation. The RVE is chosen such that there is no particle exposed on its surface S. Consequently, the matrix stiffness $\boldsymbol{C}^0$ can be applied to evaluate the traction over the entire RVE surface S.

The overall elastic stiffness of the RVE/composite, $C_{pqp'q'}$ is defined by

$$d\langle \sigma_{pq} \rangle = C_{pqp'q'} d\langle \varepsilon_{p'q'} \rangle, \quad (14)$$

where $d\langle \varepsilon_{p'q'} \rangle$ and $d\langle \sigma_{pq} \rangle$ are increments of the effective strain and the effective stress, respectively. Since the system is linear, $C_{pqp'q'}$ is a constant. Based on Equations (6) and (11), an increment of remote straining, $d\varepsilon_{st}^{\infty}$, would result in

$$d\langle \varepsilon_{p'q'} \rangle = d\varepsilon_{p'q'}^{\infty} + \sum_n I_{p'q'gh}^{*(n)} T_{ghst}^{(n)} d\varepsilon_{st}^{\infty}, \quad (15)$$

$$d\langle \sigma_{pq} \rangle = C_{pqst}^0 d\varepsilon_{st}^{\infty} + C_{pquv}^0 \sum_n J_{uvgh}^{*(n)} T_{ghst}^{(n)} d\varepsilon_{st}^{\infty}. \quad (16)$$

Finally, by realizing the fact that $d\varepsilon_{st}^{\infty}$ is arbitrary, the above three equations yield the overall stiff-

ness as

$$
\begin{aligned}
C_{pqp'q'} = & \left(C^0_{pqst} + C^0_{pquv} \sum_n J^{*(n)}_{uvgh} T^{(n)}_{ghst} \right) \\
& \cdot \left(\delta_{p's}\delta_{q't} + \sum_n I^{*(n)}_{p'q'gh} T^{(n)}_{ghst} \right)^{-1} . \quad (17)
\end{aligned}
$$

The above tensors, $\mathbf{I}^*$ and $\mathbf{J}^*$, which are integrals of the less-defect GF, contain the effect of long-range interaction between particles. The tensor, $\mathbf{T}$ describes the short-range effect of local shape and elastic properties of a particle, equivalent to the Eshelby's tensor. If the defect GF in Equations (7) and (13) are replaced by the reference GF, $\mathbf{G}$, the formulation is reduced to the classical Eshelby's method (Eshelby, 1961; Mura, 1987), where the effect of particle interaction is ignored. It may also be reduced to the case of pair-particle interaction (Moshovidis and Mura, 1975; Yin and Sun, 2004), triple-particle interaction, etc., similar to the treatment of interaction between atoms by using pair and many-body potentials.

4 Analytical Results and Discussion

Given the experimental dimensions observed for NGPs in polymer, Equation (17) is applied to evaluate the overall elastic property of NGP nanocomposites. The polymeric matrix is epoxy, which is assumed to be isotropic and linearly elastic with Young's modulus E equal to 2.6 GPa and Poisson's ratio ν equal to 0.35. The graphite platelets are assumed to be disk-like. The diameter and thickness are set to be 400 nm and 100 nm, respectively, according to the experimental measurements as shown in Figures 1b and 2. Other aspect ratios will also be simulated for comparison. The c-axis of the graphite sheet is normal to the disk plane. The linear elastic constants of the transversely isotropic graphite platelets (Kelly, 1981) are given by $C_{11} = 1060$ GPa, $C_{12} = 180$ GPa, $C_{13} = 15$ GPa, $C_{33} = 36.5$ GPa, and $C_{44} = 2.25$ GPa, with x_3 taken to be along the c-axis. The particles are stiffer in all directions than the matrix.

First the present defect GF method is verified in the case of a regular lattice of particles where the full-field solution is available. A simulation is carried out with a total of 729 graphite platelets. The platelets are distributed on a $9 \times 9 \times 9$ simple cubic lattice. Their c-axes are all oriented along one of the base axes of the cubic lattice, e.g. (001). First, the overall elastic constants are evaluated on a RVE of various numbers of particles around the central one of the cubic lattice, from $1 \times 1 \times 1$ to $5 \times 5 \times 5$. The results are nearly invariant with sampling volume size, as may be expected in the case of periodic, uniformly oriented particles. The composite overall is of the tetrahedral anisotropy, holding six independent elastic constants. Then, the overall elastic constants are evaluated with various lattice spacings, i.e. various volume fractions. The results are plotted against volume fraction f in Figure 5. In addition, the equivalent problem of a unit cell of one particle is solved numerically by using a BE method (Brebbia et al., 1984). The effective stiffness over the unit cell is obtained under a fixed displacement boundary condition prescribed according to the strain field of one nonzero component (meanwhile the other components are equal to zero). The results as well as the predictions by the classical Eshelby's method are included in Figure 5 for comparison. The Eshelby's method considers no particle interaction effect at all in evaluating the overall property.

From Figure 5, it is seen that the prediction by the present defect GF method matches very well with the full-field solution by the numerical BE method for volume fraction f within about 10 %. The BE solution fully takes into account the effect of particle interaction and finite-size. Beyond 10 % of volume fraction, the two predictions start to deviate from one another. While the BE numerical model is trustworthy, the present defect GF model seems to predict inaccurately, especially, on the elastic constant C_{12} at the large volume fractions. A careful examination shows that when a graphite platelet is placed in the matrix under a remote straining ε_{11} with all other components equal to zero, it tends to suppress that component of straining due to its much higher stiffness in that direction than the matrix but to induce some positive straining in the transverse directions at the location of particle. This effect
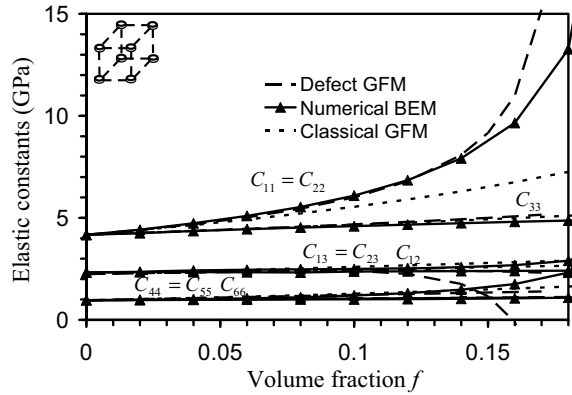
Figure 5: Variation of elastic constants with volume fraction f for composite of platelets uniformly (001)-orientated and distributed on a regular cubic lattice. The dashed lines indicate the solution of the present defect GF method. The solid lines with symbols indicate the solution of the numerical BE method. The dotted lines indicate the solution by the classical Eshelby's method.

is well balanced by the Poisson's effect in the surrounding matrix material at the small volume fractions. When the volume fraction increases, this effect grows and becomes eventually out of control due to the assumption of point-like particles. This phenomenon appears as well at volume fraction of about 45 % in the Eshelby's model prediction. Second, the Eshelby's method predicts an overall elastic stiffness systematically lower than the true value. The difference increases dramatically with increasing volume fraction when the effect of particle interaction intensifies. Therefore, the present defect GF model is validated for small volume fractions within 10 % in the case of disks of diameter-to-thickness ratio equal to 4 and distributed on a cubic lattice. This number varies with aspect ratio and arrangement of particles. Hopefully, if the finite-size effect of neighboring particles can be taken into account, the present method based on defect GF can improve to predict well the overall elastic property at higher volume fractions.

The present method employing defect GF takes into account the effect of particle interaction on the overall composite behavior. It enables us to simulate a composite system with various parti-

cle patterns and to examine the effects. To show the effect of particle distribution and orientation, the previous model system is modified by uniformly re-orientating the graphite platelets into the (111) direction of the lattice. It is equivalent to change the previous simple cubic lattice system to a BCC one where the graphite platelets are more loosely packed in the graphite basal plane. The overall elastic constants are evaluated and transformed in the coordinate system with z-axis along the particle c-axis. The results are plotted with the previous ones in Figure 6. It is shown that the re-orientation of particles leads to a remarkable change in the dominant elastic constant, i.e., C_{11} ($=C_{22}$), in the basal plane. It is understood as a result of particle interaction effect because the disk-like particles now are more loosely arranged with longer distance in the basal plane than previously, which is the strongest stiffening direction by the graphite platelets. Therefore, the particle arrangement, including both special distribution and orientation, may play a significant role in determining the overall elastic property due to the effect of particle interaction in graphite platelet composites.
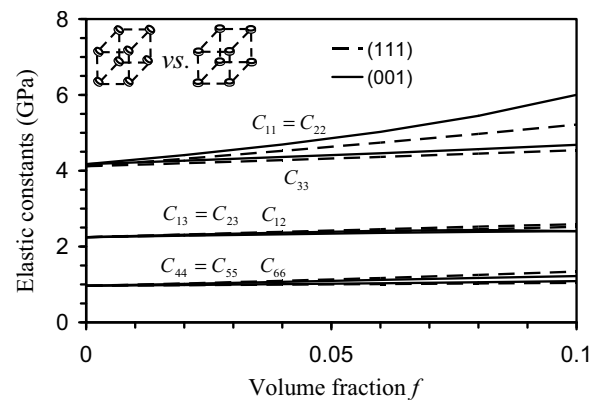
Figure 6: Variation of elastic constants with volume fraction f for composite of platelets uniformly (111)-orientated and distributed on a regular cubic lattice, compared to the results from Figure 5.

To further show the effect of particle arrangement, a random system of graphite platelets is simulated. The platelets are randomly distributed as well as randomly orientated, both with equal

probability in the space. The overall elastic property is found to converge with increasing sampling volume size. It is (nearly) isotropic as expected. The results, obtained with a RVE of 729 platelets windowed in the middle of a volume of 2197 platelets, are shown in Figure 7. The corresponding results taking into account no effect of particle interaction are also shown in the figure for comparison. It is seen that the effect of particle interaction is trivial in this case. Previously it has been shown that the graphite platelets interact strongly with each other when they are aligned in their *c*-axis and on top of one another. The effect decreases when either condition is altered. Therefore, in the case of randomly distributed and randomly oriented platelets, the effect of particle interaction in total disappears.
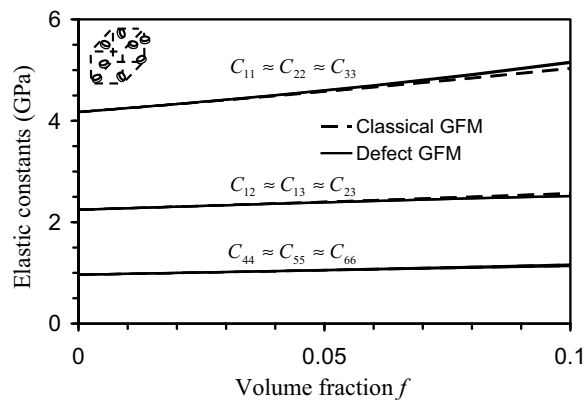
Figure 7: Variation of elastic constants with volume fraction *f* for composite of platelets randomly oriented and randomly distributed. The solids lines indicate the solution of the present defect GF method. The dashed lines indicate the solution of the classical Eshelby's method.

It has been well understood that the aspect ratio of particles/fibers plays a significant role in determining the overall property of composites (Mura, 1987). To show this effect quantitatively in the case of graphite platelets, a couple of simulations are run with different aspect ratios. The previous simulation is repeated with platelets of radius-to-thickness ratio equal to 4:1 and 6:1. Since the material overall is isotropic, the Young's modulus and Poisson's ratio are used instead in the following discussion. The results together with that of

the previous case are plotted in Figure 8. It is seen that the Poisson's ratio does not change much with aspect ratio of particles while the Young's modulus increases. By increasing the platelet aspect ratio, the stiffening effect would be very much enhanced, nearly linearly.
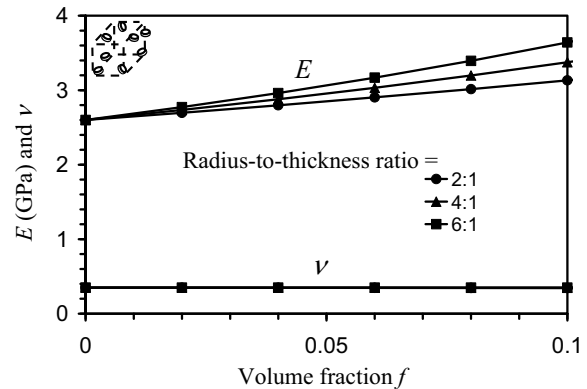
Figure 8: Variation of Young's modulus and Poisson's ratio with volume fraction *f* for composite of randomly oriented and randomly distributed platelets of various aspect ratios.

The interfacial condition between particles and matrix material is important in transferring load and thus affects the overall property of composites (Liu et al., 2005). This is even more important than ever in developing nanocomposites due to its large surface-to-volume ratio. Another simulation is done to show how the stiffness of a thin layer of interphase material between particles and matrix plays a role in determining the overall behavior of composite. A thin layer 10 nm thick is wrapped around the graphite platelets, simulating a transition zone between the particles and the bulk matrix material. It is assumed that imperfect bonding may exist that causes a softer interphase in average. For Young's modulus of the interphase equal to 1, 0.5, 0.2 and 0.1 of that of the bulk matrix, the overall elastic constants of composite with randomly distributed and randomly oriented particles are calculated and plotted in Figure 9. It is seen that the stiffening effect of graphite platelets quickly drops and diminishes when the "bonding" layer softens. Note that the simulation was done under tensile loading. If the loading is compressive, closing of the soft layer

needs to be considered, which would significantly change the results. It may be worth mentioning that a cohesive zone model may be applied to the thin layer to simulate progressive damage around the particles. In the present formulation, it may be done with interaction effect taken into account in a large system of particles. This may facilitate a way of investigating how the particle patterns determine the overall composite toughness as well as various intrinsic length scales involved in the multiscale damage process. It would be impossible without taking into account the particle interaction effect.
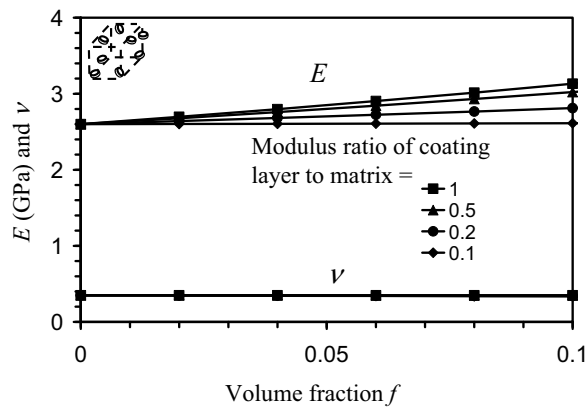
Figure 9: Variation of Young's modulus E and Poisson's ratio v with volume fraction f for composite of randomly oriented and randomly distributed platelets coated with a layer of various ratios of modulus to the bulk matrix.

5   Conclusions

A novel micromechanics model has been developed to estimate the overall elastic property of particle-reinforced composites with effect of particle interaction taken into account. This is done by employing the defect GF in the presence of all particles. The particles are assumed to be point-like. Thus, the model is applicable to the case of small volume fractions of particles (within 10 %). In particular the method has been applied to examine the nanoscale graphite platelets epoxy composites. It is a novel material system that may lead to various important applications. The particles are modeled as disk-like. First of all, the

present model is verified with a comparison of its prediction with the full-field solution in the case of a regular lattice of particles. The comparison demonstrates that it is a considerable improvement over the classical Eshelby's method employing the regular GF and hence neglecting/ignoring the effect of particle interaction. Then, a number of simulations are carried out to examine the effects of various parameters, including particle distribution, orientation, platelet aspect ratio, and a bonding layer. It is found that the effect of particle arrangement is in general significant due to the interaction of particles. The particle interaction effect is the strongest in the case when the graphite platelets are orientated uniformly and stacked one above another. However, when the platelets are randomly orientated, the overall particle interaction effect diminishes. The effect of platelet aspect ratio is significant. Finally, a soft bonding layer is inserted to simulate a partial bonding condition, between particles and matrix material. It plays a significant role in determining the overall elastic property of the composite. The present study establishes a framework for modeling particle interaction in composites. One extension in progress is to model particles undergoing damage with interaction. Also the study provides insight and guidance to experimental investigations of nanoscale graphite platelets composites. It will be cross-examined by optimized materials processing in the future work.

References

Barsukov, I.V.; Zaleski, P.L. (2004): *Method of preparing graphite intercalation compounds and resultant products*. US Patent 6756027.

Brebbia, C.A.; Telles, J.C.F.; Wrobel, L.C. (1984): *Boundary Element Techniques: Theory and Applications in Engineering*. Springer-Verlag, New York.

Budiansky, B.; Wu, T.T. (1962): Theoretical prediction of plastic strains of polycrystals. *Proceedings of 4ᵗʰ U.S. National Congress of Applied Mechanics*, 1175-1185.

Cao, N.Z.; Shen, W.C.; Wen, S.Z.; Liu, Y.J.; Wang, Z.D.; Inagaki, M. (1996): The factors influencing the porous structure of expanded graphite. *Mater. Sci. Eng.* (Chinese) 14, 22-26.

Chung, D.D.L. (1987): Exfoliation of graphite. *J. Mater. Sci.* 22, 4190-4198.

Dong, M.; Schmauder, S. (1996): Modeling of metal matrix composites by a self-consistent embedded cell model. *Acta Mater.* 44, 2465-2478.

Eshelby, J.D. (1961): Elastic inclusions and inhomogeneities, in: I.N. Sneddon and R. Hill (eds.), *Progress in Solids Mechanics* 2, North-Holland, Amsterdam, 89-140.

Fornes, T.D.; Paul, D.R. (2003): Modeling properties of nylon 6/clay nanocomposites using composite theories. *Polymer* 44, 4993-5013.

Giannelis, E.P.; Krishnamoorti, R.; Manias, E. (1999): Polymer-silicate nanocomposites: model systems for confined polymers and polymer brushes. *Adv. Polym. Sci.* 138, 107-147.

Gong, X.; Liu, J.; Baskaran, S.; Voise, R.D.; Young, J.S. (2000): Surfactant-assisted processing of carbon nanotube/polymer composites. *Chem. Mater.* 12, 1049-1052.

Jang, B.Z.; Yang, L.; Wong, S.C.; Bai, Y. (2004): *Process for producing nano-scaled graphene plates.* US Patent Application 20050271574.

Kelly, B.T. (1981): *Physics of graphite*, Appl Sci Publ Ltd, Barking, England.

Kojima, Y.; Usuki, A., Kawasumi, M.; Okada, A.; Kurauchi, T.; Kamigaito, O. (1993): Synthesis of nylon 6-clay hybrid by montmorillonite intercalated with -caprolactam. *J. Polym. Sci., Part A: Polym. Chem.* 31, 983-986.

Li, J.; Kim, J.K.; Sham, M.L. (2005): Conductive graphite nanoplatelet/epoxy nanocomposites: Effects of exfoliation and UV/ozone treatment of graphite. *Scripta Mater.* 53, 235-240.

Liu, D.S.; Chen, C.Y.; Chiou, D.Y. (2005): 3-D modeling of a composite material reinforced with multiple thickly coated particles using the infinite element method. *CMES: Computer Modeling in Engineering and Sciences* 9, 179-191.

Liu, Y.J.; Nishimura, N.; Otani, Y.; Takahashi, T.; Chen, X.L.; Munakata, H. (2005): A fast boundary element method for the analysis of fiber-reinforced composites based on a rigid-inclusion model. *J. Appl. Mech.* 72, 115-128.

LLorca, J.; Segurado, J. (2004): Three-dimensional multiparticle cell simulations of deformation and damage in sphere-reinforced composites. *Mater. Sci. Engin.* A365, 267-274.

Moshovidis, Z.A.; Mura, T. (1975): Two elliptical inhomogeneities by the equivalent inclusion method. *J. Appl. Mech.* 42, 847-852.

Mura, T. (1987): *Micromechanics of Defects in Solids.* Martinus Nijhoff, Boston.

Nemat-Nasser, S.; Hori, M. (1999): *Micromechanics: Overall Properties of Heterogeneous Materials.* 2ⁿᵈ ed., Elsevier Science, Netherlands.

Okada, H.; Liu, C.T.; Ninomiya, T.; Fukui, Y.; Kumazawa, N. (2004): Analysis of particulate composite materials using an element overlay technique. *CMES: Computer Modeling in Engineering and Sciences* 6, 333-348.

Pan, E.; Yang, B.; Cai, G.; Yuan, F.G. (2001): Stress analyses around holes in composite laminates using boundary element method. *Engineering Analysis with Boundary Elements* 25, 31-40.

Qu, S.; Wong, S.C. (2005): Piezoresistive behavior of polymer reinforced by expanded graphite. *Composite Science and Technology*, submitted.

Sau, M.; Jana, S.C. (2004): A study on the effects of chaotic mixer design and operating conditions on morphology development in immiscible polymer systems. *Polym. Engg. Sci.* 44, 407-422.

Thostenson, E.T.; Chou, T.W. (2002): Aligned multi-walled carbon nanotube-reinforced composites: processing and mechanical characterization. *J. Phys. D: Appl. Phys.* 35, L77-L80.

Thostenson, E.T.; Chou, T.W. (2003): On the elastic properties of carbon nanotube-based composites: Modelling and characterization. *J. Phys. D: Appl. Phys.* 36, 573-582.

Toyoda, M.; Inagaki, M. (2000): Heavy oil sorp-

tion using exfoliated graphite: New application of exfoliated graphite to protect heavy oil pollution. *Carbon* 38, 199-210.

Wong, S.C.; Sutherland, E.M.; Uhl, F.M. (2006): Materials processes of graphite nanostructured composites using ball milling. *Materials and Manufacturing Processes* 20, 159-166.

Wong, S.C.; Sutherland, E.M.; Yerramaddu, S.; Wouterson, E.M.; Uhl, F.M.; Webster, D.C. (2004): Processing and properties of graphene-based nanocomposites. *Proceedings of IMECE04*, 2004 ASME International Mechanical Engineering Congress and Exposition.

Wong, S.C.; Wouterson, E.M.; Sutherland, E.M. (2005): Dielectric properties of graphite nanocomposites. *Proceedings of the 63rd Annual Technical Conference of the Society of Plastics Engineers*.

Wong, S.C.; Yang, B. (2005): Piezoresistive behavior and elastic deformation of nanoscale graphite platelet reinforced polymers. PMSE Preprints, *American Chemical Society Division of Polymeric Materials: Science and Engineering, 230th ACS National Fall Meeting*, vol. 93, 210-212.

Wu, Y.P.; Jia, Q.X.; Yu, D.S.; Zhang, L.Q. (2004): Modeling Young's modulus of rubber-clay nanocomposites using composite theories. *Polym. Test* 23, 903-909.

Yang, B. (2004): Defect Green's function of multiple point-like inhomogeneities in a multilayered anisotropic substrate. *J. Appl. Mech.* 71, 672-676.

Yang, B.; Tewary, V.K. (2004): Continuum Dyson's equation and defect Green's function in a heterogeneous anisotropic solid. *Mech. Res. Commun.* 31, 405-414.

Yin, H.; Sun, L.; Paulino, G.H. (2004): Micromechanics-based elastic model for functionally graded materials with particle interactions. *Acta Mater.* 52, 3535-3543.

Yoshida, A.; Hishiyama, Y.; Inagaki, M. (1991): Exfoliated graphite from various intercalation compounds. *Carbon* 29, 1227-1231.

Zheng, W.; Lu., X.; Wong, S.C. (2004): Electrical and mechanical properties of expanded graphite-reinforced high-density polyethylene. *J. Appl. Polym. Sci.* 91, 2781-2788.

Zheng, W.; Wong, S.C. (2003): Electrical conductivity and dielectric properties of PMMA/expanded graphite composites. *Comp. Sci. Tech.* 63, 225-235.

Zheng, W.; Wong, S.C.; Sue, H.J. (2002): Transport behavior of PMMA/expanded graphite nanocomposites. *Polymer* 43, 6767-6773.

Zhu, L.; Narh, K.A. (2004): Numerical simulation of the tensile modulus of nanoclay-filled polymer composites. *J. Polym. Sci. B: Polym Phys* 42, 2391-2406.